Bio-Design and Manufacturing (2024) 7:624–636
https://doi.org/10.1007/s42242-024-00289-z

RESEARCH ARTICLE

Ionic liquid-based transparent membrane-coupled human lung epithelium-on-a-chip demonstrating PM0.5 pollution effect under breathing mechanostress

Bilgesu Kaya[1] · **Ozlem Yesil-Celiktas**[1,2]

Received: 2 August 2023 / Accepted: 14 May 2024 / Published online: 2 August 2024

Abstract

The plausibility of human exposure to particulate matter (PM) has witnessed an increase within the last several years. PM of different sizes has been discovered in the atmosphere given the role of dust transport in weather and climate composition. As a regulator, the lung epithelium orchestrates the innate response to local damage. Herein, we developed a lung epithelium-on-a-chip platform consisting of easily moldable polydimethylsiloxane layers along with a thin, flexible, and transparent ionic liquid-based poly(hydroxyethyl) methacrylate gel membrane. The epithelium was formed through the culture of human lung epithelial cells (Calu-3) on this membrane. The mechanical stress at the air–liquid interface during inhalation/exhalation was recapitulated using an Arduino-based servo motor system, which applied a uniaxial tensile strength from the two sides of the chip with 10% strain and a frequency of 0.2 Hz. Subsequently, the administration of silica nanoparticles (PM0.5) with an average size of 463 nm to the on-chip platform under static, dynamic, and dynamic + mechanical stress (DMS) conditions demonstrated the effect of environmental pollutants on lung epithelium. The viability and release of lactate dehydrogenase were determined along with proinflammatory response through the quantification of tumor necrosis factor-α, which indicated alterations in the epithelium.

✉ Ozlem Yesil-Celiktas
ozlem.yesil.celiktas@ege.edu.tr

[1] Department of Bioengineering, Faculty of Engineering, Ege University, Izmir 35100, Türkiye

[2] Translational Pulmonary Research Center (EgeSAM), Ege University, Izmir 35100, Türkiye

Graphic abstract

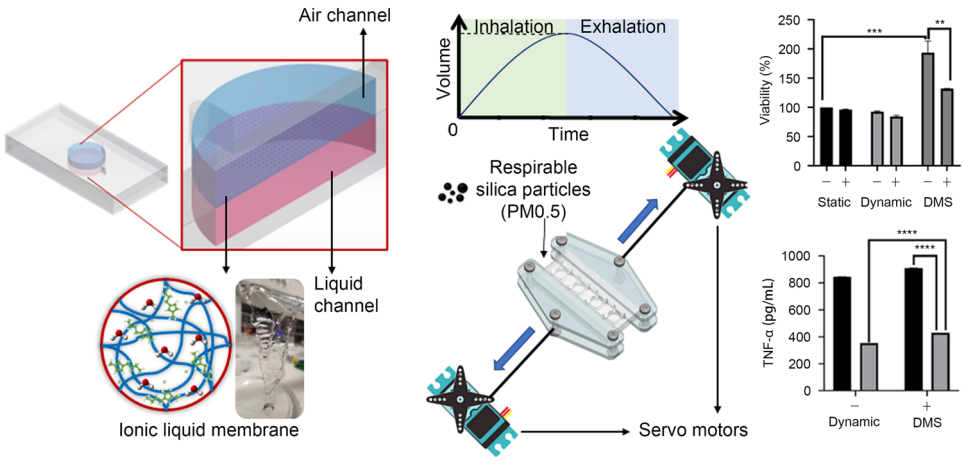

Keywords Ionic liquid-based membrane · Lung · Epithelial barrier · Mechanostress · Organ-on-chip · Silica particles

Introduction

The accuracy and precision of preclinical phases of drug development processes increase the effectiveness and success rate of drug candidates. In vitro two-dimensional (2D)/three-dimensional (3D) cell culture procedures [1, 2], ex vivo [3] and in vivo animal models [4] have been used in the screening of potential molecules, where successful candidates in preclinical settings continue to be investigated in clinical studies on humans. However, these models fail to yield physiologically relevant responses of the human body against administered molecules. In this context, alternative systems must be developed to improve preclinical processes. Organs-on-chips, which have gained a considerable interest, allow the investigation of human physiological/immunological responses without ethical concerns [5] and reduce the use of animals [6]. The human lung is a vital respiratory organ that participates in metabolic activities, such as gas exchange, acid–base balance, and blood pressure regulation. Global warming and climate change have adverse effects on respiratory health [7], along with the increased use of detergents/surfactants, processed foods, nanoparticles, and microplastics [8]. Especially, particulate matter (PM) less than 2.5 μm damages tight junction proteins, particularly those in the lung epithelium, which leads to exposure time- and dose-dependent acute/chronic respiratory diseases [9]. Thus, intense research efforts have been aimed at modeling these pathologies via epithelium-on-a-chip platforms [10] to accelerate the clinical translation of promising therapeutics. A recent study delved into the importance of epithelial barrier in addressing other global health concerns. This investigation utilized a lung-on-a-chip model to assess the effect of severe acute respiratory syndrome coronavirus 2 (SARS-CoV-2) at the organ level. Through the cultivation of human alveolar epithelial cells and lung microvasculature cells in adjacent channels separated by a porous membrane in an on-chip platform, the researchers successfully replicated the virus's interaction with the mentioned specific cell types [11]. Another study focused on growing stratified epithelia on a commercial E-transflow device comprised of a culture well with a microfluidic channel via a porous membrane to correlate the Stokes radius and molecular diffusion through the epithelium [12]. However, an in vitro model representing the lung epithelium without mechanostress proved to be insufficient for the accurate prediction of the effects of such pollutants. Therefore, scholars have shifted their focus on the development of biomimetic on-chip platforms that recapitulate the mechanical [13] and physiological properties which epithelial cells are exposed to [10]. This raises another concern regarding the synthesis of membranes to be integrated into the organ-on-a-chip platforms for the formation of the air–liquid interface. Various porous and stretchable membranes have been integrated into on-chip platforms; such membranes include polydimethylsiloxane (PDMS) [14, 15], polyester [16], polyurethane [17], polycarbonate [18], bacterial cellulose [19], and collagen–elastin [20]. Ionic liquids as conductive hydrogels have drawn research attention lately [21, 22] in the field of biomedical technology. However, they have not been used in the recapitulation of barriers in organ-on-a-chip platforms. Thus, to bridge this gap, we synthesized and characterized a lung epithelium-on-a-chip platform consisting of easily moldable PDMS layers along with a thin, flexible, transparent, and ionic liquid-based hydrophilic poly(hydroxyethyl) methacrylate (pHEMA) gel

membrane (PH-GM). The epithelium was formed by culturing human lung epithelial cells (Calu-3) on the membrane under mechanical stress, which occurred at the air–liquid interface during the inhalation/exhalation mechanism through recapitulation by an Arduino-based servo motor system (torque of 4.8 V: 10 kgf·cm). The system applied uniaxial tensile strength from two sites on the chip with 10% strain and a frequency of 0.2 Hz. Subsequently, PM0.5 (i.e., silica nanoparticles) was administered to the on-chip platform to assess the effect of environmental pollutants on lung epithelium under emulated inhalation/exhalation.

Materials and methods

Materials

1-Butyl-3-methylimidazolium chloride (BmimCl) was purchased from ACROS Organics (Geel, Belgium) and 2-hydroxyethyl methacrylate (HEMA) from Aldrich Chemistry (St. Louis, Missouri, USA). Fibronectin, laminin, proteoglycan, potassium persulfate (KPS), tetramethylethylenediamine (TEMED), and Dulbecco's modified Eagle's medium/Ham's F-12 (1:1) (DMEM/F-12) were bought from Sigma-Aldrich Co., Ltd (St. Louis, Missouri, USA). Collagen A, glutaraldehyde, sodium cacodylate and ethanol (100%) were secured from Merck Co., Ltd (Rahway, New Jersey, USA), and penicillin/streptomycin was purchased from Biosera (Cholet, France). PDMS base solution and curing agent (SYLGARD 184) were used.

Synthesis of ionic liquid-based pHEMA membrane

The preparation of pHEMA-based hydrogels involved the replacement of BmimCl in the polymer network with water after in situ free-radical polymerization of HEMA monomers in water and ionic liquid (BmimCl) mixed solutions, in accordance with the protocol optimized by Liu et al. [23]. Within the scope of the protocol, a homogeneous precursor solution was prepared containing BmimCl and water at the weight ratio of 2:8. A total of 3.9 g HEMA (0.03 mol) was added to the water/BmimCl mixture. The water/BmimCl/HEMA mixture was kept in a nitrogen atmosphere for 5 min at 80 °C. A total of 0.5 g KPS solution (0.02 g/mL) and 8 μL TEMED were added to the precursor and served as redox initiators. To accurately maintain the thickness of the resultant membrane, we strategically interposed the preexisting PDMS layers with a standardized thickness of 100 μm between the curing slides at both ends of the mold. Subsequently, the precursor was molded and left at room temperature for 48 h to enable free-radical polymerization. This procedural measure was implemented to guarantee that the membrane, which was formed upon the introduction of the uncured solution between slides, maintained a 100 μm thickness. The resultant hydrogels (containing ionic liquid) were retained in distilled water to remove BmimCl in the bonds. The gels with thicknesses of 100 μm were named as PH-GM.

Characterization

Tensile test

Uniaxial tensile test was applied to determine the mechanical properties of PH-GMs, which formed the surface on which cells attached and acted as a membrane in the microchips.

Scanning electron microscopy (SEM) imaging

For SEM, the samples were fixed using three different buffers. First, the samples were fixed using 2.5% glutaraldehyde in 0.1 mol/L cacodylate buffer for 30 min at 4 °C, immersed in 1.4% (0.014 g/mL) sucrose solution in sodium cacodylate buffer, and postfixed for 30 min in a 1% osmium tetroxide solution in 0.1 mol/L sodium cacodylate buffer. The membranes were dehydrated at room temperature in 35%, 50%, 70%, 85%, 95%, and 100% ethanol for 5 min each. Finally, the samples were immersed in hexamethyldisilane for 5 min and dried overnight at room temperature. After drying, the samples were placed on brass carriers, coated with 200 Å-thick (1 Å $= 10^{-10}$ m) gold, and examined under a scanning electron microscope.

Water contact angle

Contact angle measurement qualitatively assesses the hydrophobicity or hydrophilicity property of a surface. This process is based on the observation of intermolecular interactions between the surface and water droplet when they come into contact. Contact angle measurement is mainly used to evaluate surface wettability. This characterization technique is used to analyze whether the hydrophilic surface required for cell attachment is provided in the produced gel membrane. The samples were washed with deionized water, transferred on a slide at room temperature, and placed in the contact angle device while drying. Approximately 4 μL liquid was dropped onto the membrane surface, and the angle between the contact surface and the drop was photographed using the camera system and then measured using SCA20.2.0 software (firmware version 2.05). Measurements were taken through the analysis of different samples in at least three repetitions. Analysis was also conducted on the PH-GMs to be used in the microfluidic platform and PDMS membranes as a comparison group.

Residual mass analysis for degradation assessment

In residual mass analysis, the synthesized PH-GMs were kept in DMEM/F-12 nutrient medium for 7 d. Mass loss was calculated by measuring the dry weights on Days 0, 1, 4, and 7.

Breathing mechanostress in lung epithelium-on-a-chip

Simulation

SolidWorks was applied in the simulation of strain and displacement changes under the mechanical stress that the microplatform and PH-GMs were exposed to. To obtain results close to the physiological conditions in the cell culture environment, we adjusted the ambient temperature to 37 °C. SolidWorks program was also applied in the mechanical stress system created with servo motors to observe stress/displacement simulations and the effects of the strain to which the chip and membrane were exposed and analyze the deformation of the produced membrane. In the simulations, the chip and the membrane, which were subjected to force to ensure 1 mm expansion of the 10-mm-wide PH-GM, were analyzed. In the simulation performed through the application of a fixed fixture to one side, the mesh was created with a global dimension value of 0.28509647 mm and a tolerance value of 0.01425482 mm based on standard parameters. The temperature was set at 37 °C, and 10% strain was obtained by applying a force of 0.39 N. The stress results were expressed in terms of von Mises stress, which is calculated to determine whether the structure has undergone plastic deformation under any loading condition. Displacement results were obtained in millimeters, in accordance with the definition of URES (Resultant Displacement) in SolidWorks simulation.

Design and fabrication

Molds were designed using SolidWorks 3D computer-aided design program for the fabrication of the microchip platform and mechanical stress system. Separate drawings were prepared for the air/liquid layers and the polymethyl methacrylate (PMMA) plates to be used in the adaption of the chip to the mechanical stress system. The molds were produced by cutting the PMMA plates into the required thickness using a desktop laser cutting device (VLS2.30 System Universal Laser). The microplatform consisted of top–bottom layers of biocompatible PDMS and biocompatible PH-GM of the working chip. To emulate the mechanical stress, we compressed the microplatform using four PMMA plates, with two plates on each side, and integrated it into the system to adapt them to the traction system consisting of two servo motors (Tower Pro MG995). The dimensions of the chamber for cell culture in the working chip were designed to mimic the circular alveolar structure with surface areas of 10 mm × 10 mm × 2 mm and 0.785 mm^2. The mechanical stress platform was based on the principle of pulling two servo motors axially to the PDMS chip compressed with PMMAs to simulate mechanical stress. The gel revealed a stretch, which was applied in a loop with a frequency of 0.2 Hz, imitating the breathing mechanism of an adult human. The equation in Scheme 1 can be applied to create 10% strain of the axial tension applied to ionic liquid-based PH-GMs [24].

Scheme 1 Equation applied to create 10% strain of the axial tension applied to ionic liquid-based PH-GMs. PH-GMs: poly(hydroxyethyl) methacrylate gel membranes

Formulation of the lung epithelium

Surface modification of the membrane to improve cell adhesion

Cell adhesion was optimized by coating the surface of PH-GMs with a protein cocktail prior to cell culture. Two different procedures were applied for surface modification. In the first application, a phosphate buffered saline (PBS) solution of 5 μg/cm^2 fibronectin was prepared and added to the chamber for cell culture and aerated for 45 min at room temperature. Then, the liquid was removed from the chamber. In the other application, a solution was prepared with PBS containing laminin, fibronectin, collagen A, and proteoglycan at 5 μg/cm^2 concentration and applied to the gel surface. After 2 h at 37 °C, the liquid was removed, and the chamber was washed with PBS.

Seeding epithelial cells

Calu-3 cells used to establish the epithelial barrier were utilized on the platform by thawing cells with passage number 9 from the stocks. In the thawing process, cell-containing cryotubes were removed from the liquid nitrogen tank and placed in a water bath, which was previously set at 37 °C to thaw up to 75%. Afterward, 1 mL freezing medium containing 90% fetal bovine serum and 10% dimethyl sulfoxide was added to the tubes placed in a laminar air-flow cabinet with biosafety level 2. The mixture of cells and freezing medium was pipetted completely and transferred to a centrifuge tube, which was then centrifuged at 4 °C and 1000 r/min for 5 min. Without damaging the collapsed cell pellet, the supernatant was removed, and the nutrient medium added to the cell pellet was thoroughly homogenized and transferred to T25

flasks. The flasks were incubated in 37 °C incubators containing 5% CO_2. The nutrient media were changed every other day, and cells were examined daily under a microscope. Cell counting and subsequent seeding were performed at 80% cell density of the attachment surface of the flasks. Cell cultivation involved removal of the nutrient medium and several times of gentle cell washing using the PBS solution. After the removal of the PBS solution, 0.25 mL and 0.75 mL trypsin-ethylenediaminetetraacetic acid solutions were separately added to the T25 and T75 flasks, respectively, to lift cells from the surface. After microscopic observation, the cells were scraped from the flask to ensure complete cell suspension. Then, for the neutralization and subsequent removal of the trypsin solution, the cell-containing liquid was collected from the flask, transferred to a separate centrifuge tube, and added with 4 mL nutrient medium. The tube was centrifuged at 4 °C and 1000 r/min for 5 min, the supernatant was removed, and the cells were counted. Calu-3 cells were cultured on the upper surface of the PH-GM embedded in the epithelium-on-a-chip platform at a concentration of 2×10^5 cells/mL. The chips were placed on the rocker and shaken at 1 r/min to obtain dynamic ambient conditions.

Viability of epithelial cells

A quantitative analysis method WST-1 was used to analyze the viability of cells cultured on the platform. The nutrient medium was removed from the PH-GMs with cell attachment and washed with PBS. The nutrient medium solution containing 10:1 WST-1 was prepared in a total volume of 65 μL for each chamber. The solution was added to the chambers containing the cells, and incubation was performed at 37 °C and 5% CO_2 for 3 h away from the light. After incubation, the supernatants were collected from the chambers and transferred to wells in a 96-well plate. The plate was placed on a microplate reader in the absence of light and spectrophotometrically analyzed at a wavelength of 450 nm. Viability calculations were performed using GraphPad Prism 8.0.

Administration of PM0.5 to lung epithelium-on-a-chip

Characterization and administration of PM

Silica particles purchased from Dost Kimya, Türkiye, were ground and filtered by filters of 1 μm pore size. The particle size distribution and zeta potential were measured (Zetasizer Nano ZS, Malvern Panalytical, UK) through the selection of a refractive index of 1.50 and absorption value of 0.001, which are specific to silica. The particles suspended in DMEM/F-12 were centrifuged (10,000 r/min and 15 min), and the pellet was dispersed in distilled water and sonicated (Ultrasonic Cleaners, Everest Ultrasonic, CleanEx-812) for 20 min to prevent aggregation. Subsequently, 1 mL sample was loaded into a micro cuvette to measure the particle size distribution, and another sample was loaded into a folded capillary zeta cell (DTS1070, Malvern Panalytical) using a syringe to measure the zeta potential. PM0.5 silica particles (800 μg/mL) were applied to lung epithelium-on-a-chip to assess the sensitivity of the model. Experiments were conducted under three conditions. In static conditions, the cell culture medium was not circulated, and the on-chip system was not exposed to mechanical stress. In dynamic conditions, mechanical stress was not applied, and the cell culture medium was circulated via a rocker. In DMS conditions, mechanical stress was applied, and the cell culture medium was circulated.

Immunofluorescence imaging

4′,6-Diamidino-2-phenylindole immunofluorescence staining was performed on lung epithelial cells for the qualitative analysis of the effect of mechanical stress on cells.

Viability of epithelial cells

WST-1 assay was performed as described previously to determine the viabilities of epithelial cells exposed to PM0.5 at a concentration of 800 μg/mL under static, dynamic, and DMS conditions.

Proinflammatory response

The level of human tumor necrosis factor alpha (TNF-α), which represents the proinflammatory response after silica application, was determined using double-antibody sandwich enzyme-linked immunosorbent assay (ELISA). Supernatants obtained from the cells were diluted at the ratio of 5:1 with a sample dilution solution and placed in 96-well plates that were previously coated with TNF-α monoclonal antibody. The plates were incubated at 37 °C for 90 min. After incubation, 100 μL biotin-labeled antibody solution was added to the wells that were washed twice and incubated at 37 °C for 60 min. Then, 100 μL horseradish peroxidase–streptavidin conjugate solution was added to the wells removed from incubation, washed thrice, and incubated at 37 °C for 30 min. Afterward, washing was performed five times for 2 min each time with a washing solution to remove unbound enzymes. After the addition of 90 μL TMB substrate to each well, the mixture was mixed gently and incubated at 37 °C for 10–20 min protected from light. After incubation, 50 μL stop solution was added to each well. The color turned yellow quickly, and the absorbances of the samples were immediately read on the microplate reader at the wavelength of 450 nm.

Results and discussion

Synthesis of ionic liquid-based pHEMA membrane and characterization

The breathing mechanism of the lung and the resultant mechanical stress acting on cells are vital in the investigation of organ-on-a-chip platforms, where flexible materials such as PDMS are used [25]. In a recent study, the fabrication of thin PDMS films involved the spinning and coating of polymers on a wafer. The thickness and plasticity of PDMS films obtained at different spinning speeds were determined, and the obtained results demonstrated that the 100-μm-thick PDMS films were highly elastic and thus can withstand sustained cycles of expansion and contraction in lung-on-a-chip platforms [26]. In another study, 81.4% elongation of PDMS membrane was observed on the lung-on-a-chip at break point [27]. Although the body of our platform is made up of PDMS, the synthesized PH-GM (Fig. 1a) had a thickness of 100 μm and was sandwiched in between two PDMS layers. Thus, not only PDMS but also the membrane must be elongated to withstand cyclic mechanical stress. The PH-GMs were elongated by 265% until the breaking point (Fig. 1b), indicating the potential of ionic liquid-based membranes for mechanical stress applications. Moreover, a high porosity is required for the membranes used in organ-on-chips for the controlled transport of various nutrients and increased cell adhesion [28]. The membranes produced using different materials, such as polyethylene terephthalate, polyester, polycarbonate, and PDMS, can have varying pore diameters; the desired sizes can be obtained through fabrication methods such as soft lithography [29, 30]. In a recent study, the polycarbonate membranes used for lung-on-a-chip had pore sizes of 0.4–0.8 μm [18].

As displayed in the SEM image, PH-GMs showed a high porosity with pore diameters in the range of 0.15–0.17 μm (Fig. 1c). Water contact angle can also be used to evaluate the degree of hydrophilicity, which is a critical parameter for the adhesion and proliferation of cells that grow via attachment in in vitro cell culture systems [14, 15]. During the examination of surface hydrophilicity, PH-GMs exhibited a high hydrophilicity with an average contact angle measurement of approximately 43.02°, whereas PDMS exerted hydrophobic properties with an average contact angle measurement of around 101.68° (Figs. 1d and 1e). As the surface properties of biomaterials influence cell behavior, including cell adhesion, orientation, and migration [31], PH-GM is an ideal candidate due to its hydrophilic nature. Degradation

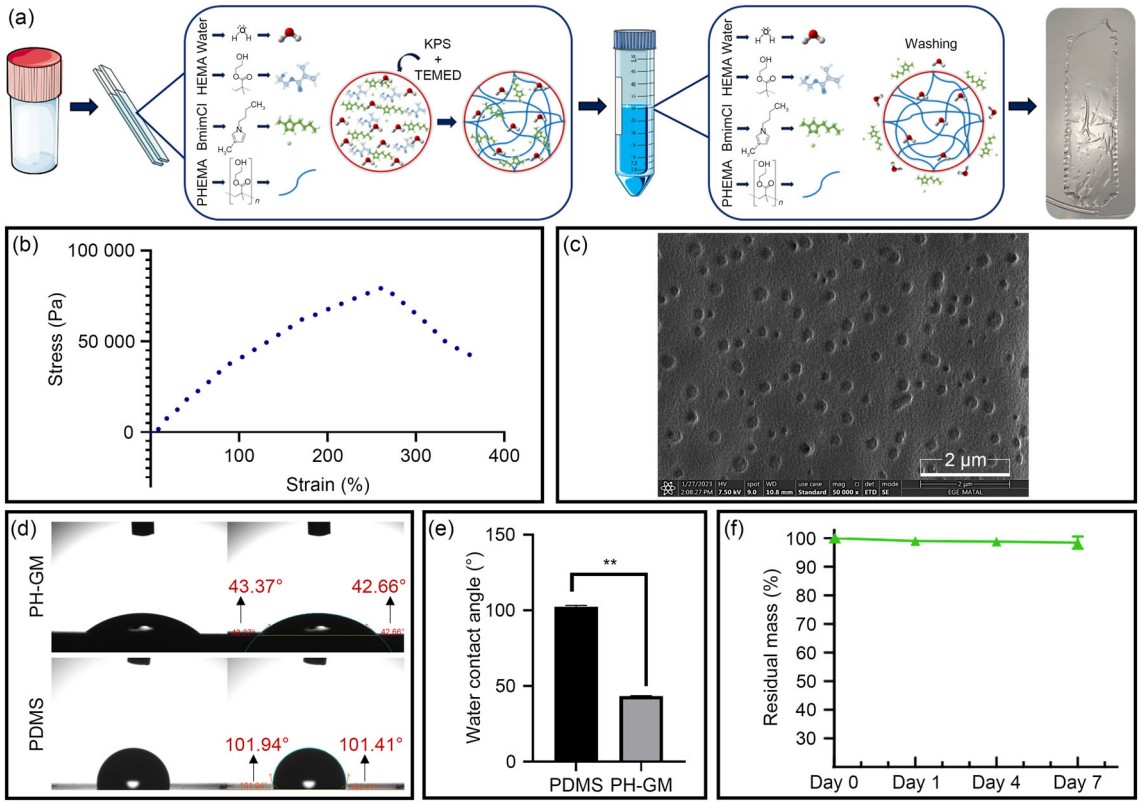

Fig. 1 **a** Schematic of ionic liquid-based membrane fabrication; **b** tensile strength; **c** scanning electron micrograph of the pores; **d**, **e** water contact angle of ionic liquid-based PH-GM compared with that of PDMS; **f** residual mass analysis of PH-GMs for degradation assessment. PH-GM: poly(hydroxyethyl) methacrylate gel membrane; PDMS: polydimethylsiloxane

analysis revealed that PH-GMs degraded to a small extent (2%) when kept in DMEM/F-12 nutrient medium at 37 °C for 7 d (Fig. 1f). Biodegradability is an important criterion in tissue engineering applications, and a low percentage of degradation is more effective for the establishment of long-lived cell cultures in organ-on-chips. Overall, the transparency, high porosity, hydrophilicity, slow degradation, and high elongation of PH-GMs favor their utilization as a barrier mimicking membrane.

Breathing mechanostress in lung epithelium-on-a-chip

Cells are not exposed to physiological mechanical signals, including shear stress, strain/compression, and specific dimensional and geometric nanostructures, during the application of conventional cell culture methods. However, these signals are involved in physiological processes from tissue morphogenesis [32] to organ development, which are missing in 2D models, in addition to cell proliferation [33]. For this reason, in vitro cultures must also include the mechanical conditions that cells are exposed to in the microenvironment. Thus, we selected appropriate components for the design of the lung epithelium-on-a-chip platform to recapitulate physiological mechanical cues. These mechanical signals, including displacement and strain, were simulated using SolidWorks. The displacement simulations showed the same elongation mechanism of the PDMS chambers (Fig. 2a) and PH-GM (Fig. 2b) under an axially applied force.

The elongation reached 1 mm on average in the middle part, where the top and bottom chambers separated by the PH-GM (diameter: 10 mm) represented the air–liquid interface, and the strain rate of the PH-GM was 10%, according to the strain equation [34]. In the strain simulation carried out to observe material deformation under an applied force, the PDMS chambers (Fig. 2c) and PH-GM (Fig. 2d) did not stretch up to the yield strength level of 7×10^5 N/m^2 and returned to their former form when the applied force was removed [35]; thus, the combination of PDMS and ionic liquid-based PH-GM can ideally emulate the inhalation/exhalation mechanism. Following simulation studies, fabrication of the designed PDMS-based microplatform was accomplished by molding (Fig. 2e), and the mechanical stress (pull) system developed (Fig. 2f) based on Arduino-based servo motors was integrated into the microplatform to emulate the inhalation/exhalation mechanism (Fig. 2g) in the lungs. Different from that of other studies currently available,

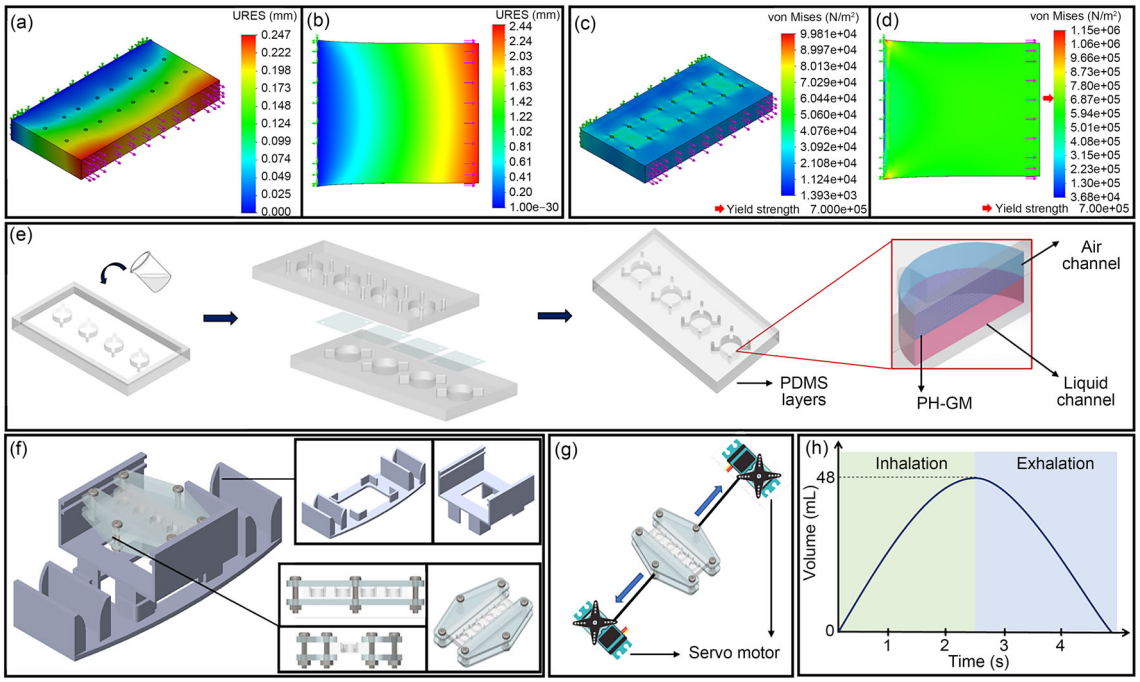

Fig. 2 **a** Simulation of microchip for displacement in millimeters; **b** simulation of ionic liquid-based PH-GM for displacement in millimeters; **c** simulation of microchip for strain depicted by von Mises plot (N/m^2); **d** simulation of PH-GM for strain depicted by von Mises plot (N/m^2); **e** fabrication of the PDMS-based microchip, **f** mechanical stress system, **g** working principle of the servo motor system used to stretch the 10-mm-long PH-GM by 1 mm to provide 10% strain to exert the appropriate torque (4.8 V: 10 kgf·cm); **h** illustrational graph of inhalation/exhalation in human lungs. PH-GM: poly(hydroxyethyl) methacrylate gel membrane; PDMS: polydimethylsiloxane; URES: Resultant Displacement (in SolidWorks simulation)

the design is based on the principle of pulling the chip axially as a whole (Fig. 2h) and not by vacuum application to the membranes [14, 20]. The assembled microplatform enabled for the adjustment of the desired strain value by changing the rotation angle and cycle duration of the servo motors, which provided a convenient system for the investigation of various mechanical stress applications.

Formulation of the lung epithelium

After microplatform assembly, the lung epithelium was formulated, where Calu-3 epithelial cells derived from human bronchial submucosal glands [36] were utilized as the submucosal glands, which are a major source of airway surface liquid, mucins, and other immunologically active substances; Calu-3 cells reflect these properties [37, 38]. However, different cell culture media were used for the cultivation of Calu-3 cells [39, 40]. Thus, we tested the efficacies of three different cell culture media, including DMEM/F-12, DMEM high glucose, and Roswell Park Memorial Institute (RPMI) 1640 nutrient medium, and observed them for 8 d (Fig. S1 in Supplementary Information). Calu-3 cells exhibited better epithelial morphologies and proliferation rates in DMEM/F-12 nutrient medium. Apart from elicitation of the medium, the surface properties of membranes are pivotal for cell attachment and confluency. Routinely, special surface coatings, such as fibronectin and collagen, are used in maintenance of a physiologically relevant surface for cells [41].

The PH-GMs exhibited highly hydrophilic properties, and thus, we coated their surface with fibronectin and a protein cocktail composed of laminin, fibronectin, collagen A, and proteoglycan (Fig. 3a) to enhance their adhesive properties. An identical number of Calu-3 cells were seeded, and the results showed that proliferation was improved on protein cocktail-coated PH-GMs compared with those coated by fibronectin and non-coated cells (Fig. 3b). Finally, the viability of Calu-3 cells seeded on protein cocktail-coated PH-GMs was tested under static, dynamic, and DMS conditions. No statistically significant difference was observed in cell viabilities under static and dynamic conditions. However, viability was significantly improved under DMS conditions (Fig. 3c), where the only difference was observed in the mechanical stress applied axially at a frequency of 0.2 Hz, that is, the emulation of the breathing mechanism of an adult human. Cells activate different signaling pathways due to exposure to mechanical forces, which may occasionally cause apoptosis or induce cell growth [42]. The physical integrity of the epithelial cell monolayer is regulated by the force balance at the cell–cell and cell–matrix attachments [43]. Under physiological conditions, epithelial cells bear a state of internal tension, which is counterbalanced by outward adhesive forces that tether cells to one another and the extracellular matrix [44]. However, this is not a static balance of forces. Lung cells continuously experience cyclic stretching. Thus, the proliferation of Calu-3 cells under DMS conditions might have been improved due to the cellular responses that can withstand the increased elastic recoil induced by stretching.

Administration of PM0.5 to lung epithelium-on-a-chip

Finally, we tested the effect of PM0.5 on the lung epithelium-on-a-chip (Fig. S2 in Supplementary Information) by administering silica particles with an average diameter of 463 nm and zeta potential value of − 28.2 mV at a concentration of 800 μg/mL (Fig. 4a) under static, dynamic, and DMS conditions. We transferred 65 μL silica solution to each chamber to expose the cells to approximately 52 μg silica. According to epidemiological and clinicopathological studies, silica dust-associated pathological changes are characterized by inflammation and progressive fibrosis [45]. The international recommended exposure limit is 50 $\mu g/m^3$, which is a time-weighted average for up to 10 h per day during a 40-h week [46]. A silica concentration above 2000 $\mu g/m^3$, which was accidentally observed in a Scottish colliery in the 1970s, is three times more effective in silicosis production than concentrations below such level [47]. Thus, short-term exposures to high concentrations of silica, which results in such pathological conditions, may be attributed to the high proportion of silica particles in respirable dust. During the evaluation of immunofluorescent stained images, the effect of PM0.5 was more prominent under dynamic conditions compared with that under static conditions (Fig. 4b), which was proven by cell deformation and the disruption of nuclear structures. The cellular uptake of polystyrene nanoparticles was investigated on a lung-on-a-chip platform under mechanical stress. The results showed that when 10% tension was applied, the cellular uptake of polystyrene nanoparticles was considerably increased compared with that under static conditions [15]. In our study, the cell viabilities under static conditions showed no significant variation with (96.13%) or without (100%) silica application, whereas a slight decrease occurred under dynamic conditions after PM0.5 exposure (from 92.90% to 84.52%). However, an approximately 1.5-fold decrease was noted in cell viability (from 193.87% to 131.94%) under DMS conditions, which suggested a similar trend subsequent to PM0.5 exposure. Thus, mechanical stress increased the penetration of silica particles and enabled them to cause further damage on the cell structure. Light microscopy images (Fig. 4c) and the viabilities of Calu-3 cells (Fig. 4d) revealed that the higher effect of PM0.5 exposure was observed on cells cultured under DMS conditions compared with those under dynamic and static conditions. A study focused on the interactions between silica particles and model phospholipid monolayers, and the results showed that PM with diameters less than 10 μm exerted a negative effect

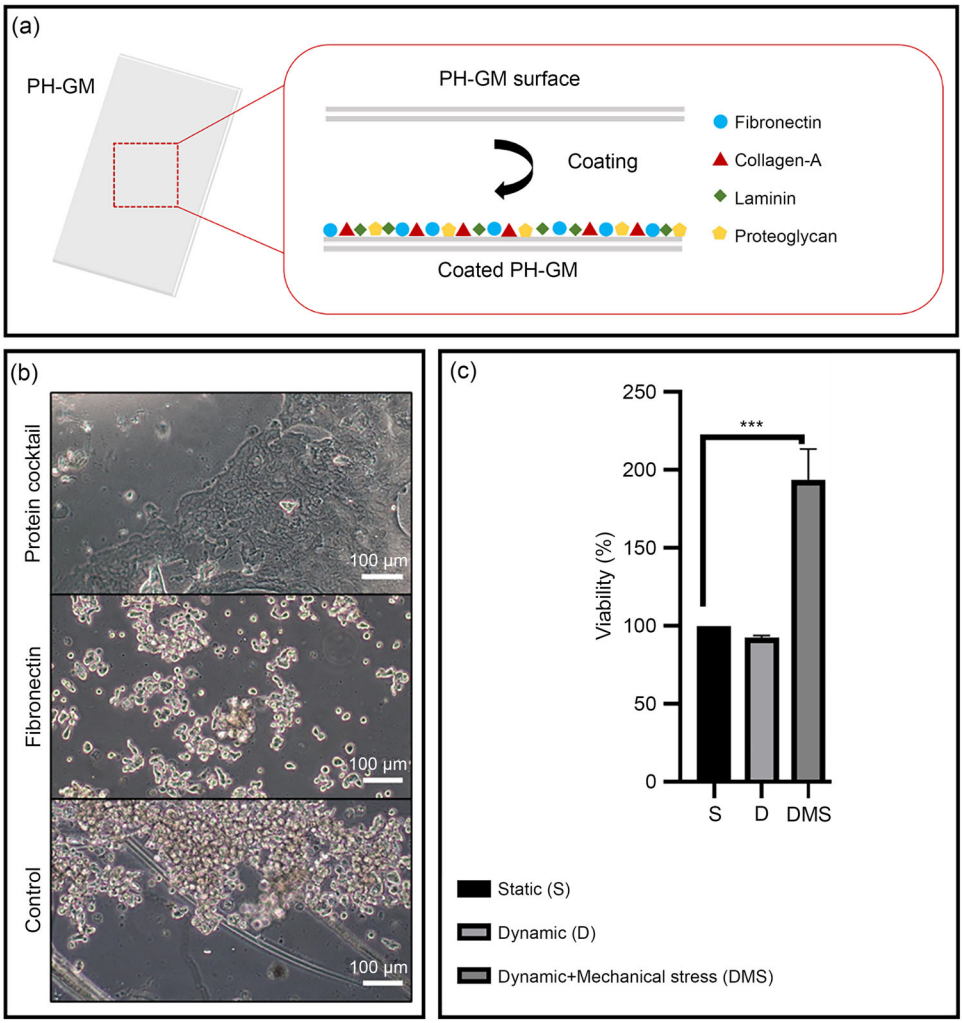

Fig. 3 **a** Surface modification on PH-GM with protein cocktail. **b** Comparison of surface modification with fibronectin and protein cocktail with 20× magnification; scale bar: 100 µm. **c** Viability assessment of Calu-3 cells under static, dynamic, and DMS conditions ($n = 3$ for independent replicates; one-way ANOVA Tukey's multiple comparisons test; $^{***}p < 0.001$). PH-GM: poly(hydroxyethyl) methacrylate gel membrane; ANOVA: analysis of variance

on the lipid membrane morphology [48]. The effects of various micro/nanoparticles present in the biosphere were also examined using lung epithelial cells seeded with MucilAir™ inserts. Despite the varied levels of cytotoxic effects based on the type of micro/nanoparticles, 5%–10% cytotoxicities were observed, most probably owing to static culture conditions [49], which justified the necessity of advanced in vitro models. A study evaluating the effects of mechanical strain utilized A549 cells as a model for alveolar epithelial cells and exposed them to 25 nm amorphous colloidal silica nanoparticles under dynamic and static culture conditions. Gene array data, quantitative polymerase chain reaction, and ELISA results revealed the amplified effect of nanoparticles during mechanical stretching of cells for modeling physiological mechanical deformation during breathing [50].

Exposure to PM also initiates proinflammatory cell activation, with TNF-α as one of the proinflammatory cytokines [51] with signaling pathways that simultaneously regulate cell apoptosis and proliferation [52]. Considering the lung epithelium, bronchial epithelial cells are among the first cells exposed to inhaled irritants, and they can initiate innate immune responses to these exposures through the release of proinflammatory cytokines, including TNF-α [53]. Furthermore, TNF-α initiates proinflammatory signaling in pathologies induced by silica [54]. Although large crystalline silica particles influence biological responses through proinflammatory mediators, small silica nanoparticles may traverse the airway barrier, enter the systemic circulation, and directly affect secondary organs [55]. Therefore, changes in TNF-α expression under dynamic and DMS conditions with and without PM0.5 administration were investigated (Fig. 4d). The presence of silica induced TNF-α release in both conditions. Interestingly, the release of TNF-α from Calu-3 cells under DMS conditions with cyclic stretching was 50% less compared with that under dynamic conditions. One study analyzed the production of proinflammatory cytokines in the lungs during high mechanical stretching in vivo. The high mechanical ventilation did not cause the release of proinflammatory cytokines (TNF-α and interleukin-1β) into the air spaces of isolated rat lungs. As such, TNF-α release

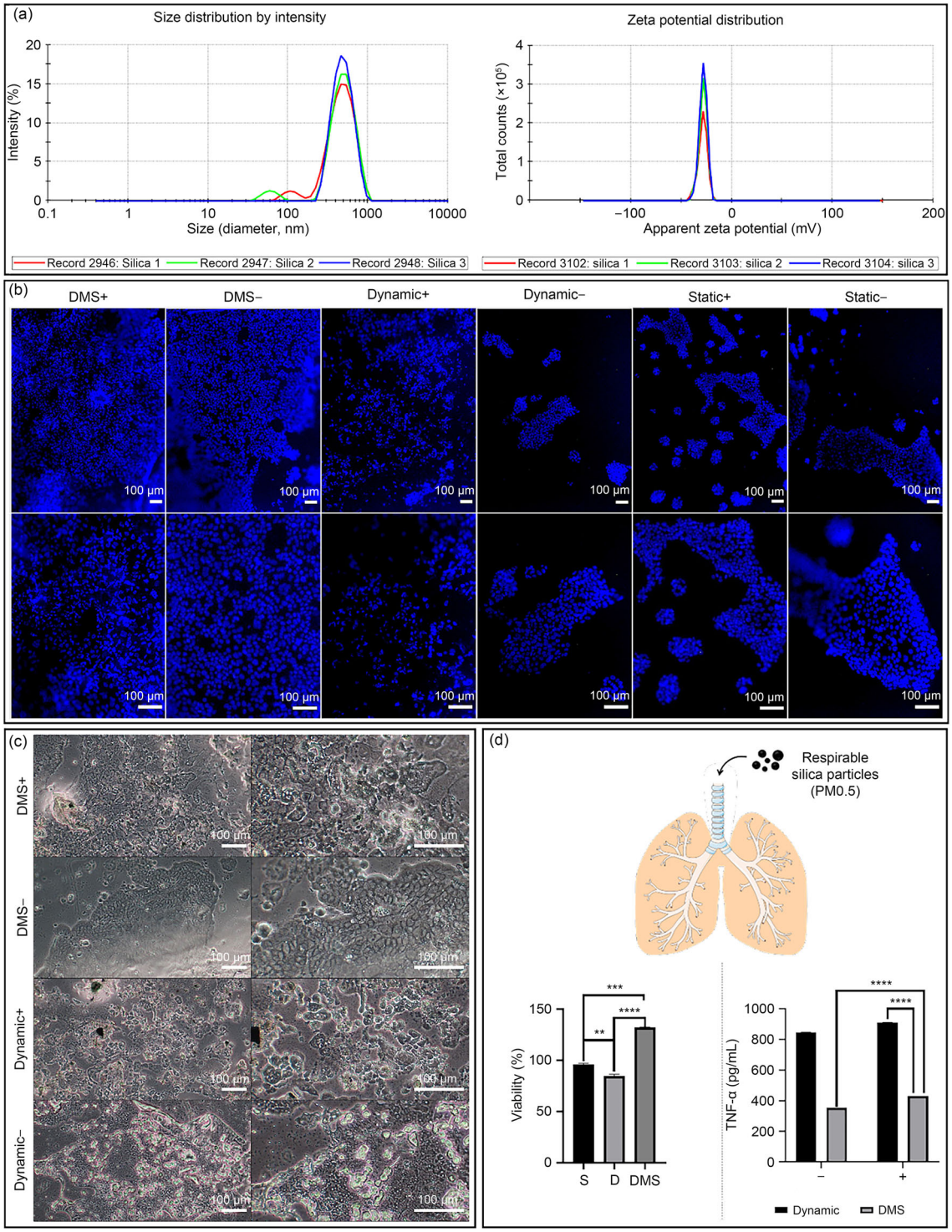

Fig. 4 **a** Size distribution and zeta potential of PM0.5. **b** Immunostaining images of Calu-3 cells under DMS, dynamic, and static conditions with (+) and without (−) PM0.5 administration at 10× (upper panel) and 20× (lower panel) magnifications; scale bar: 100 μm. **c** Light microscopy images of cells at 10× (left) and 20× (right) magnifications; scale bar: 100 μm. **d** Viabilities (%) of Calu-3 cells with (+) and without (−) PM0.5 exposure under static, dynamic, and DMS conditions and proinflammatory analysis of TNF-α ($n = 3$ for independent replicates; one-way ANOVA Tukey's multiple comparisons test; $^{**}p < 0.01$, $^{***}p < 0.001$, and $^{****}p < 0.0001$; the image was generated using Servier Medical Art, which was provided by Servier, and licensed under a Creative Commons Attribution 3.0 unported license). DMS: dynamic + mechanical stress; S: static; D: dynamic; TNF-α: tumor necrosis factor alpha; ANOVA: analysis of variance

did not occur in the air spaces of the lungs or in the systemic circulation of animals, even in the case of pulmonary edema formation under high ventilation conditions [56]. Although the administration of PM0.5 resulted in considerably increased concentrations of TNF-α under DMS conditions, the presence of mechanical stress decreased its expression, thus providing a desirable biomimetic model.

Conclusions

Studies are devoting considerable efforts to the exploration of the effects of fine PM, especially PM2.5 and PM10, on human respiratory system due to the increased air pollution, which is closely linked to climate change. Therefore, the assessment of the toxic effects caused by these PMs should include the assistance provided by physiologically relevant in vitro models. In this study, we developed a lung epithelium-on-a-chip consisting of PDMS layers and a thin, flexible ionic liquid-based PH-GM seeded with human lung epithelial cells. The susceptibility of the lung epithelium to static, dynamic, and DMS conditions was evaluated by administering the PM0.5 to the on-chip platform. The viability of Calu-3 cells was improved, and the cytotoxicity of PM0.5 was more prominent under DMS conditions. In addition, the mechanical forces at the air–liquid interface during the inhalation/exhalation mechanism revealed in vivo-like properties, as observed in the TNF-α response, indicating the importance of biomimicry. Consequently, the developed lung epithelium-on-a-chip can be utilized for the toxicity assessment of various micro/nanoparticles.

Supplementary Information The online version contains supplementary material available at https://doi.org/10.1007/s42242-024-00289-z.

Acknowledgements BK acknowledges the TUBITAK 2210-C National Graduate Scholarship Program and access to the laboratory of Prof. Dr. Sinan Akgol at Biochemistry Department of Ege University. This work was supported by the Presidency of the Republic of Türkiye Strategy Budget Department (2019K12-149080).

Author contributions BK was involved in conceptualization, investigation, methodology, visualization, data curation, and writing of the original draft; OYC contributed to conceptualization, provided supervision, and was involved in writing, reviewing, and editing.

Funding Open access funding provided by the Scientific and Technological Research Council of Türkiye (TÜBİTAK).

Declarations

Conflict of interest The authors declare that they have no conflict of interest.

Ethical approval This study does not contain any studies with human or animal subjects performed by any of the authors.

References

1. Fontoura JC, Viezzer C, dos Santos FG et al (2020) Comparison of 2D and 3D cell culture models for cell growth, gene expression and drug resistance. Mater Sci Eng C 107:110264. https://doi.org/10.1016/j.msec.2019.110264
2. Saygili E, Devamoglu U, Goker-Bagca B et al (2022) A drug-responsive multicellular human spheroid model to recapitulate drug-induced pulmonary fibrosis. Biomed Mater 17(4):045021. https://doi.org/10.1088/1748-605X/ac73cd
3. Saglam-Metiner P, Yildiz-Ozturk E, Tetik-Vardarli A et al (2024) Precision cut lung slices as a preclinical model to study host-influenza A infection. Tissue Cell 87:102319. https://doi.org/10.1016/j.tice.2024.102319
4. Butler KS, Brinker CJ, Leong HS (2022) Bridging the in vitro to in vivo gap: using the chick embryo model to accelerate nanoparticle validation and qualification for in vivo studies. ACS Nano 16(12):19626–19650. https://doi.org/10.1021/acsnano.2c03990
5. Hou W, Hu SY, Yong K et al (2020) Cigarette smoke-induced malignant transformation via STAT3 signalling in pulmonary epithelial cells in a lung-on-a-chip model. Bio-Des Manuf 3(4):383–395. https://doi.org/10.1007/s42242-020-00092-6
6. Saygili E, Yildiz-Ozturk E, Green MJ et al (2021) Human lung-on-chips: advanced systems for respiratory virus models and assessment of immune response. Biomicrofluidics 15(2):021501. https://doi.org/10.1063/5.0038924
7. Cooper DM, Loxham M (2019) Particulate matter and the airway epithelium: the special case of the underground? Eur Respir Rev 28(153):190066. https://doi.org/10.1183/16000617.0066-2019
8. Amato-Lourenço LF, Carvalho-Oliveira R, Júnior GR et al (2021) Presence of airborne microplastics in human lung tissue. J Hazard Mater 416:126124. https://doi.org/10.1016/j.jhazmat.2021.126124
9. Zhang L, Wang CS, Xian M et al (2020) Particulate matter 2.5 causes deficiency in barrier integrity in human nasal epithelial cells. Allergy Asthma Immunol Res 12(1):56–71. https://doi.org/10.4168/aair.2020.12.1.56
10. Lin LN, Wang XC, Niu MY et al (2022) Biomimetic epithelium/endothelium on chips. Eng Regen 3(2):201–216. https://doi.org/10.1016/j.engreg.2022.05.001
11. Zhang M, Wang P, Luo RH et al (2021) Biomimetic human disease model of SARS-CoV-2-induced lung injury and immune responses on organ chip system. Adv Sci 8(3):2002928. https://doi.org/10.1002/advs.202002928
12. Fernandez-Carro E, Salomon-Cambero R, Armero L et al (2023) Nanoparticles Stokes radius assessment through permeability coefficient determination within a new stratified epithelium on-chip model. Artif Cell Nanomed B 51(1):466–475. https://doi.org/10.1080/21691401.2023.2253534

13. Melo-Fonseca F, Carvalho O, Gasik M et al (2023) Mechanical stimulation devices for mechanobiology studies: a market, literature, and patents review. Bio-Des Manuf 6(3):340–371. https://doi.org/10.1007/s42242-023-00232-8
14. Stucki AO, Stucki JD, Hall SRR et al (2015) A lung-on-a-chip array with an integrated bio-inspired respiration mechanism. Lab Chip 15(5):1302–1310. https://doi.org/10.1039/c4lc01252f
15. Huh D, Matthews BD, Mammoto A et al (2010) Reconstituting organ-level lung functions on a chip. Science 328(5986):1662–1668. https://doi.org/10.1126/science.1188302
16. Benam KH, Villenave R, Lucchesi C et al (2016) Small airway-on-a-chip enables analysis of human lung inflammation and drug responses in vitro. Nat Methods 13:151–157. https://doi.org/10.1038/nmeth.3697
17. Niu MY, Zhu YJ, Ding XY et al (2023) Biomimetic alveoli system with vivid mechanical response and cell–cell interface. Adv Healthc Mater 12(26):e2300850. https://doi.org/10.1002/adhm.202300850
18. Baptista D, Moreira Teixeira L, Barata D et al (2022) 3D lung-on-chip model based on biomimetically microcurved culture membranes. ACS Biomater Sci Eng 8(6):2684–2699. https://doi.org/10.1021/acsbiomaterials.1c01463
19. Saygili E, Devamoglu U, Bayir E et al (2023) An optical pH-sensor integrated microfluidic platform multilayered with bacterial cellulose and gelatin methacrylate to mimic drug-induced lung injury. J Ind Eng Chem 121:190–199. https://doi.org/10.1016/j.jiec.2023.01.023
20. Zamprogno P, Wüthrich S, Achenbach S et al (2021) Second-generation lung-on-a-chip with an array of stretchable alveoli made with a biological membrane. Commun Biol 4(1):168. https://doi.org/10.1038/s42003-021-01695-0
21. Hong Y, Lin ZN, Luo ZR et al (2022) Development of conductive hydrogels: from design mechanisms to frontier applications. Bio-Des Manuf 5(4):725–756. https://doi.org/10.1007/s42242-022-00208-0
22. Jing YF, Wang AH, Li JL et al (2022) Preparation of conductive and transparent dipeptide hydrogels for wearable biosensor. Bio-Des Manuf 5(1):153–162. https://doi.org/10.1007/s42242-021-00143-6
23. Liu YW, Wang P, Wang J et al (2020) Transparent and tough poly(2-hydroxyethyl methacrylate) hydrogels prepared in water/IL mixtures. New J Chem 44:4092–4098. https://doi.org/10.1039/d0nj00214c
24. Roan E, Waters CM (2011) What do we know about mechanical strain in lung alveoli? Am J Physiol Lung Cell Mol Physiol 301(5):L625–L635. https://doi.org/10.1152/ajplung.00105.2011
25. Tan JF, Sun XD, Zhang JH et al (2022) Exploratory evaluation of EGFR-targeted anti-tumor drugs for lung cancer based on lung-on-a-chip. Biosensors 12(8):618. https://doi.org/10.3390/bios12080618
26. Zhu YJ, Sun LY, Wang Y et al (2022) A biomimetic human lung-on-a-chip with colorful display of microphysiological breath. Adv Mater 34(13):2108972. https://doi.org/10.1002/adma.202108972
27. Kadyrova A, Kanabekova P, Martin A et al (2022) Evaluation of membranes for mimicry of an alveolar-capillary barrier in microfluidic lung-on-a-chip devices. Mater Today Proc 71:7–12. https://doi.org/10.1016/j.matpr.2022.05.582
28. Echeverria Molina MI, Malollari KG, Komvopoulos K (2021) Design challenges in polymeric scaffolds for tissue engineering. Front Bioeng Biotechnol 9:617141. https://doi.org/10.3389/fbioe.2021.617141
29. Walter FR, Valkai S, Kincses A et al (2016) A versatile lab-on-a-chip tool for modeling biological barriers. Sensor Actuat B-Chem 222:1209–1219. https://doi.org/10.1016/j.snb.2015.07.110
30. Shrestha J, Ghadiri M, Shanmugavel M et al (2019) A rapidly prototyped lung-on-a-chip model using 3D-printed molds. Organs-on-a-Chip 1:100001. https://doi.org/10.1016/j.ooc.2020.100001
31. Agmon G, Christman KL (2016) Controlling stem cell behavior with decellularized extracellular matrix scaffolds. Curr Opin Solid State Mater Sci 20(4):193–201. https://doi.org/10.1016/j.cossms.2016.02.001
32. Saglam-Metiner P, Devamoglu U, Filiz Y et al (2023) Spatio-temporal dynamics enhance cellular diversity, neuronal function and further maturation of human cerebral organoids. Commun Biol 6(1):173. https://doi.org/10.1038/s42003-023-04547-1
33. Mousavi SJ, Hamdy Doweidar M (2015) Role of mechanical cues in cell differentiation and proliferation: a 3D numerical model. PLoS ONE 10(5):e0124529. https://doi.org/10.1371/journal.pone.0124529
34. Fuard D, Tzvetkova-Chevolleau T, Decossas S et al (2008) Optimization of poly-di-methyl-siloxane (PDMS) substrates for studying cellular adhesion and motility. Microelectron Eng 85(5–6):1289–1293. https://doi.org/10.1016/j.mee.2008.02.004
35. Peng J, Grayson M, Snyder GJ (2021) What makes a material bendable? A thickness-dependent metric for bendability, malleability, ductility. Matter 4(9):2694–2696. https://doi.org/10.1016/j.matt.2021.07.015
36. Da Paula AC, Ramalho AS, Farinha CM et al (2005) Characterization of novel airway submucosal gland cell models for cystic fibrosis studies. Cell Physiol Biochem 15(6):251–262. https://doi.org/10.1159/000087235
37. Dubin RF, Robinson SK, Widdicombe JH (2004) Secretion of lactoferrin and lysozyme by cultures of human airway epithelium. Am J Physiol Lung Cell Mol Physiol 286(4):L750–L755. https://doi.org/10.1152/ajplung.00326.2003
38. Zhu Y, Chidekel A, Shaffer TH (2010) Cultured human airway epithelial cells (Calu-3): a model of human respiratory function, structure, and inflammatory responses. Crit Care Res Pract 2010:1–8. https://doi.org/10.1155/2010/394578
39. Florea BI, Meaney C, Junginger HE et al (2002) Transfection efficiency and toxicity of polyethylenimine in differentiated Calu-3 and nondifferentiated COS-1 cell cultures. AAPS PharmSci 4(3):12. https://doi.org/10.1208/ps040312
40. Grainger CI, Greenwell LL, Lockley DJ et al (2006) Culture of Calu-3 cells at the air interface provides a representative model of the airway epithelial barrier. Pharm Res 23(7):1482–1490. https://doi.org/10.1007/s11095-006-0255-0
41. Akamatsu Y, Akagi T, Sumitomo T et al (2023) Construction of human three-dimensional lung model using layer-by-layer method. Tissue Eng Part C Methods 29(3):95–102. https://doi.org/10.1089/ten.tec.2022.0184
42. Ingber DE (2018) From mechanobiology to developmentally inspired engineering. Philos Trans R Soc B Biol Sci 373(1759):20170323. https://doi.org/10.1098/rstb.2017.0323
43. Waters CM, Roan E, Navajas D (2012) Mechanobiology in lung epithelial cells: measurements, perturbations, and responses. Compr Physiol 2(1):1–29. https://doi.org/10.1002/cphy.c100090
44. Dudek SM, Garcia JGN (2001) Cytoskeletal regulation of pulmonary vascular permeability. J Appl Physiol 91(4):1487–1500. https://doi.org/10.1152/jappl.2001.91.4.1487
45. Hnizdo E, Vallyathan V (2003) Chronic obstructive pulmonary disease due to occupational exposure to silica dust: a review of epidemiological and pathological evidence. Occup Environ Med 60(4):237–243. https://doi.org/10.1136/oem.60.4.237
46. Rumchev K, Hoang DV, Lee A (2022) Case report: exposure to respirable crystalline silica and respiratory health among Australian mine workers. Front Public Health 10:798472. https://doi.org/10.3389/fpubh.2022.798472
47. Buchanan D, Miller BG, Soutar CA (2003) Quantitative relations between exposure to respirable quartz and risk of silicosis.

Occup Environ Med 60(3):159–164. https://doi.org/10.1136/oem.60.3.159
48. Rojewska M, Tim B, Prochaska K (2022) Interactions between silica particles and model phospholipid monolayers. J Mol Liq 345:116999. https://doi.org/10.1016/j.molliq.2021.116999
49. Donkers JM, Höppener EM, Grigoriev I et al (2022) Advanced epithelial lung and gut barrier models demonstrate passage of microplastic particles. Microplast Nanoplast 2:6. https://doi.org/10.1186/s43591-021-00024-w
50. Schmitz C, Welck J, Tavernaro I et al (2019) Mechanical strain mimicking breathing amplifies alterations in gene expression induced by SiO_2 NPs in lung epithelial cells. Nanotoxicology 13(9):1227–1243. https://doi.org/10.1080/17435390.2019.1650971
51. Cakmak B, Saglam-Metiner P, Beceren G et al (2022) A 3D in vitro co-culture model for evaluating biomaterial-mediated modulation of foreign-body responses. Bio-Des Manuf 5(3):465–480. https://doi.org/10.1007/s42242-022-00198-z
52. Lai WY, Wang JW, Huang BT et al (2019) A novel TNF-α-targeting aptamer for TNF-α-mediated acute lung injury and acute liver failure. Theranostics 9(6):1741–1751. https://doi.org/10.7150/thno.30972
53. Aghapour M, Raee P, Moghaddam SJ et al (2018) Airway epithelial barrier dysfunction in chronic obstructive pulmonary disease: role of cigarette smoke exposure. Am J Respir Cell Mol Biol 58(2):157–169. https://doi.org/10.1165/rcmb.2017-0200TR
54. Malaviya R, Laskin JD, Laskin DL (2017) Anti-TNFα therapy in inflammatory lung diseases. Pharmacol Ther 180:90–98. https://doi.org/10.1016/j.pharmthera.2017.06.008
55. Raftis JB, Miller MR (2019) Nanoparticle translocation and multi-organ toxicity: a particularly small problem. Nano Today 26:8–12. https://doi.org/10.1016/j.nantod.2019.03.010
56. Ricard JD, Dreyfuss D, Saumon G (2001) Production of inflammatory cytokines in ventilator-induced lung injury: a reappraisal. Am J Respir Crit Care Med 163(5):1176–1180. https://doi.org/10.1164/ajrccm.163.5.2006053